A novel amphipathic cell-penetrating peptide based on the N-terminal glycosaminoglycan binding region of human apolipoprotein E

Takashi Ohgita, Yuki Takechi-Haraya, Ryo Nadai, Mana Kotani, Yuki Tamura, Karin Nishikiori, Kazuchika Nishitsuji, Kenji Uchimura, Koki Hasegawa, Kumiko Sakai-Kato, et al.

BBA - Biomembranes 1861 (2019) 541–549

Contents lists available at ScienceDirect

BBA - Biomembranes

journal homepage: www.elsevier.com/locate/bbamem

A novel amphipathic cell-penetrating peptide based on the N-terminal glycosaminoglycan binding region of human apolipoprotein E

Takashi Ohgita[a,1], Yuki Takechi-Haraya[b,1], Ryo Nadai[a], Mana Kotani[a], Yuki Tamura[a], Karin Nishikiori[a], Kazuchika Nishitsuji[c], Kenji Uchimura[d], Koki Hasegawa[e], Kumiko Sakai-Kato[b], Kenichi Akaji[f], Hiroyuki Saito[a,*]

[a] Department of Biophysical Chemistry, Kyoto Pharmaceutical University, 5 Misasagi-Nakauchi-cho, Yamashina-ku, Kyoto 607-8414, Japan
[b] Division of Drugs, National Institute of Health Sciences, 3-25-26 Tonomachi, Kawasaki-ku, Kawasaki 210-9501, Japan
[c] Department of Biochemistry, Wakayama Medical University, 811-1 Kimiidera, Wakayama 641-8509, Japan
[d] Unité de Glycobiologie Structurale et Fonctionnelle, UMR 8576 CNRS, Université de Lille 1, 59655 Villeneuve d'Ascq, France
[e] Center for Instrumental Analysis, Kyoto Pharmaceutical University, 1 Misasagi-Shichono-cho, Yamashina-ku, Kyoto 607-8414, Japan
[f] Department of Medicinal Chemistry, Kyoto Pharmaceutical University, 1 Misasagi-Shichono-cho, Yamashina-ku, Kyoto 607-8414, Japan

ARTICLE INFO

Keywords:
Arginine-rich peptide
Amphipathicity
Glycosaminoglycan
Lipid membrane
Cell membrane penetration

ABSTRACT

In the direct cell membrane penetration, arginine-rich cell-penetrating peptides are thought to penetrate into cells across the hydrophobic lipid membranes. To investigate the effect of the amphipathic property of arginine-rich peptide on the cell-penetrating ability, we designed a novel amphipathic cell-penetrating peptide, A2-17, and its derivative, A2-17KR, in which all lysine residues are substituted with arginine residues, based on the glycosaminoglycan binding region in the N-terminal α-helix bundle of human apolipoprotein E. Isothermal titration calorimetry showed that A2-17 variants have a strong ability to bind to heparin with high affinity. Circular dichroism and tryptophan fluorescence measurements demonstrated that A2-17 variants bind to lipid vesicles with a structural change from random coil to amphipathic α-helix, being inserted into the hydrophobic membrane interiors. Flow cytometric analysis and confocal laser scanning microscopy demonstrated the great cell penetration efficiency of A2-17 variants into CHO-K1 cells when incubated at low peptide concentrations (2 μM or less), suggesting that the increased amphipathicity with α-helix formation enhances the cell membrane penetration ability of arginine-rich peptides. Interestingly, A2-17KR exhibited lower efficiency of cell membrane penetration compared to A2-17 despite of their similar binding affinity to lipid membranes. Since high peptide concentrations (typically > 10 μM) are usually prerequisite for efficient cell penetration of arginine-rich peptides, A2-17 is a unique amphipathic cell-penetrating peptide that exhibits an efficient cell penetration ability even at low peptide concentrations.

1. Introduction

Arginine-rich peptides, such as polyarginine, Tat, and Rev, have emerged as one of the most promising carriers for delivering drug molecules, such as nucleotides, bioactive peptides, and proteins [1,2]. The paradigm that cell membranes behave as hydrophobic barriers impermeable to ionic molecules is changing because the highly cationic arginine-rich peptides are able to penetrate into cells across the membranes via energy- and receptor-independent, non-endocytic pathway at 4 °C, in which the membrane penetration is essentially physicochemical process [3–8]. Although the mechanism by which such highly cationic peptides penetrate lipid membranes is still not fully understood, the use of arginine-rich peptides is expected to lead to development of not only innovative drug carriers but also methodology to overcome the membrane barriers without cytotoxicity [9].

Since arginine-rich peptides favorably bind to negatively charged molecules, their cell membrane penetration is thought to be initiated by binding to sulfated glycosaminoglycans (GAGs) such as heparan sulfate

Abbreviations: CD, circular dichroism; CHO, Chinese hamster ovary; CLSM, confocal laser scanning microscopy; EPC, egg phosphatidylcholine; EPG, egg phosphatidylglycerol; FAM, 5(6)-carboxyfluorescein; FBS, fetal bovine serum; GAG, glycosaminoglycan; GUV, giant unilamellar vesicle; ITC, isothermal titration calorimetry; PBS, phosphate-buffered saline; SUV, small unilamellar vesicle

* Corresponding author.
E-mail address: hsaito@mb.kyoto-phu.ac.jp (H. Saito).
[1] Both authors contributed equally to this work.

https://doi.org/10.1016/j.bbamem.2018.12.010
Received 29 August 2018; Received in revised form 17 November 2018; Accepted 13 December 2018
Available online 15 December 2018
0005-2736/

and chondroitin sulfate, covalently linked to core proteins at the cell surface [10–13]. Arginine residues in arginine-rich peptides play a critical role in binding to GAGs with large favorable enthalpy attributed to the unique electrostatic interaction including multivalent hydrogen bonding of arginine residue with sulfate and carboxyl groups of GAGs [14], thereby enhancing the cell membrane penetration of peptides [15]. After the GAG binding, arginine-rich peptides are thought to follow the two distinct steps: (I) partition to cell membranes and (II) penetration into cells over the potential barrier of the hydrophobic lipid membranes. According to this model, arginine-rich peptides with high affinity for lipid membranes are expected to efficiently penetrate into cells. However, due to the fact that the binding affinity of arginine-rich peptides for lipid membranes is typically low, the role of membrane interaction in the cell penetration ability of arginine-rich peptides remains unclear.

Human apolipoprotein E is a 299-residue protein that folds into two tertiary structure domains: a 22-kDa N-terminal domain and a 10-kDa C-terminal domain linked by a hinge region [16,17]. The N-terminal domain is folded into a four-helix bundle of amphipathic α-helices, and the segment spanning residues 135–150 on helix 4 of the helix bundle is enriched in basic arginine and lysine residues that interact with LDL receptor superfamily as well as GAGs [18–20]. Interestingly, an amphipathic 20-residue peptide derived from the tandem dimer of the heparin-binding sequence (residues 141–150) of human apolipoprotein E, called A2 (LRKLRKRLLRLRKLRKRLLR), was reported to internalize into cells through heparan sulfate-dependent endocytosis [21].

Based on the GAG-binding region of human apolipoprotein E, we in this study designed a novel amphipathic cell-penetrating peptide, A2-17 (LRKLRKRLLRLWKLRKR), referring to a typical arginine-rich cell-penetrating peptide, Rev (TRQARRNRRRRWRERQR) [14], to investigate the effect of increase in amphipathicity on the cell-penetrating ability of arginine-rich peptides. We previously reported that Rev has the greater ability to penetrate directly into cells among representative arginine-rich peptides including Tat and oligoarginine [15]. We also introduced an A2-17 derivative, A2-17KR (LRRLRRRLLRLWRLRRR), by substituting all lysine residues of A2-17 with arginine residues. Using a series of physicochemical techniques, we analyzed the interaction of peptides with heparin and small unilamellar vesicles (SUVs), as a GAG and a lipid membrane models, respectively. The cell membrane penetration of peptides was also examined in Chinese hamster ovary (CHO) cell system by flow cytometric analysis and confocal laser scanning microscopy. Our results demonstrated that A2-17 variants have a strong ability to bind to GAGs as well as lipid membranes with formation of amphipathic α-helical structure, leading to the efficient cell membrane penetration. Thus, the increase in amphipathicity with α-helix-forming ability appears to be a promising strategy to enhance the cell membrane penetration of arginine-rich peptides.

2. Materials and methods

2.1. Materials

Porcine intestinal mucosa heparin (average molecular weight of 12,500) was purchased from Celsus Laboratories (Cincinnati, OH). Egg phosphatidylcholine (EPC) was purchased from Kewpie Corporation (Tokyo, Japan). Egg phosphatidylglycerol (EPG) was purchased from NOF Corporation (Tokyo, Japan). Peptides were prepared by solid phase synthesis method using Fmoc chemistry. The peptide sequences were as follow: Rev, TRQARRNRRRRWRERQR; A2-17, LRKLRKRLLRLWKLRKR; A2-17KR, LRRLRRRLLRLWRLRRR. A2-17KR is an A2-17 analogue in which 3 K, 6 K, 13 K, and 16 K were substituted by Arg residues. The amino and carboxyl termini of each peptide were acetylated and amidated, respectively. For the fluorescence labeling of peptides, the amino terminus of peptides was labeled with 5(6)-carboxyfluorescein (FAM) via glycylglycine linker. Purification of synthesized peptides was carried out by reverse-phase HPLC. The peptides were eluted with a linear gradient of acetonitrile and water containing 0.1% trifluoroacetic acid with detection at 220 nm. The purity of each eluted peptide was confirmed to be > 95% by HPLC and electrospray ionization-mass spectrometry. All other reagents were of analytical grade.

2.2. Preparation of small Unilamellar vesicles (SUVs)

SUVs were prepared as described [22]. Briefly, a dried lipid film of EPC or EPC/EPG (4/1 molar ratio) was hydrated in 10 mM Tris buffer containing 150 mM NaCl (pH 7.4) and sonicated on ice under nitrogen. After removing titanium debris, the samples were centrifuged in a Beckman 70.1 Ti rotor for 1.5 h at 15 °C at 40,000 rpm to separate any remaining large vesicles. The concentration of EPC was determined by using an enzymatic assay kit (Phospholipid C-test Wako) from Wako Pure Chemicals (Osaka, Japan).

2.3. Preparation of Giant Unilamellar Vesicles (GUVs)

GUVs were prepared as described previously [15]. Briefly, a dried lipid film of EPC/EPG (4/1 molar ratio, total lipid amount of 1 μmol) doped with equivalent molar glucose was carefully immersed in 1 mL of 10 mM Tris buffer (pH 7.4) containing 10 mM sucrose, followed by hydration without agitation for 1–2 days at 37 °C. After hydration, a bulky white cloud floating containing GUVs was harvested and centrifuged in an AR015-SC24 rotor (TOMY Seiko, Tokyo, Japan) at 10,000 rpm for 30 min at 10 °C to remove any contaminating lipid aggregates and multilamellar vesicles.

2.4. Isothermal titration calorimetry (ITC) measurements

ITC measurements were performed using an iTC200 system (Malvern Panalytical) at 25 °C in 10 mM Tris buffer containing 150 mM NaCl (pH 7.4). Peptide solution was placed in the reaction cell, and titrated with aliquots of heparin. The injections were repeated automatically under 1000 rpm stirring. Heats of dilution were determined in control experiments by injecting heparin into buffer, and the heats were subtracted from the heats determined in the corresponding peptide binding experiments. The ITC results were fitted to the one-site binding model combined with a complex formation model in Origin 7.1 (MicroCal, Northampton, MA) to obtain thermodynamic parameters as described [23,24].

2.5. Circular dichroism (CD) measurements

Far-UV CD spectra were recorded from 190 to 250 nm at 25 °C using a Jasco J-1500 spectropolarimeter (JASCO, Tokyo, Japan) with quartz cuvette of 1 mm path length. Peptide solutions (50 μg/mL) in 10 mM Tris buffer containing 150 mM NaCl (pH 7.4) in the absence and presence of heparin or SUVs were subjected to CD measurements. The results were corrected by subtracting the baseline for an appropriate blank sample. The α-helix content of peptide was determined from mean residue ellipticity [θ], expressed in degree $cm^2\,dmol^{-1}$, at 222 nm as described [25]: α-helix content (%) = $([\theta]_{222} - [\theta]_{coil}) / ([\theta]_{helix} - [\theta]_{coil}) \times 100$; $[\theta]_{helix} = -40{,}000 \times (1\text{–}2.5/n) + 100t$; $[\theta]_{coil} = 640\text{–}45t$, where $[\theta]_{222}$ is the [θ] at 222 nm, $[\theta]_{helix}$ and $[\theta]_{coil}$ are the mean residue ellipticities of the completely helical and coiled forms of the peptide, respectively. The n is the number of amino acid residues, and t is the temperature in °C.

2.6. Trp fluorescence measurements

All fluorescence measurements were carried out with a F-7000 fluorescence spectrophotometer (Hitachi, Tokyo, Japan) at 25 °C in 10 mM Tris buffer containing 150 mM NaCl (pH 7.4). Trp emission fluorescence spectra of 50 μg/mL of Rev, A2-17 or A2-17KR were

recorded from 300 to 420 nm using a 290 nm excitation wavelength in the absence and presence of heparin or SUVs. The results were corrected by subtracting the baseline for an appropriate blank sample.

Binding behaviors of the peptides to SUVs or heparin were tracked by the change in the ratio of fluorescence intensities at wavelengths associated with hydrophobic (335 nm) and hydrophilic (355 nm) tryptophan environments [26]. The binding parameters of peptides to SUVs or heparin were determined as follows [27]. The concentration of bound peptide (P_b) is calculated by $P_b = P_T\ (I_{355}/I_{335} - I_{355}/I_{335,\ 0})\ /\ (I_{355}/I_{335,\ min} - I_{355}/I_{335,\ 0})$, where P_T is total peptide concentration, and I_{355}/I_{335} and $I_{355}/I_{335,\ 0}$ are the ratios of fluorescence intensity at 355 nm to that at 335 nm for peptide in the presence and absence of SUVs or heparin, respectively, and $I_{355}/I_{335,\ min}$ represents the I_{355}/I_{335} when peptide completely binds to SUVs or heparin. Assuming that binding of peptide to the SUV surface or heparin is described by a one-site binding model, P_b/[Lipid or heparin] $= B_{max}\ P_f\ /\ (1/K + P_f)$, where P_f is unbound peptide concentration ($P_f = P_T - P_b$), [Lipid or heparin] is the concentration of phospholipid of SUVs or heparin added, and K and B_{max} are the binding constant and the maximal binding capacity, respectively. Binding data were analyzed by linear regression based on the Hanes-Woolf equation, [Lipid or heparin] $P_f/P_b = (1/K)\ /\ B_{max} + P_f/B_{max}$.

2.7. Cell culture

Wild type CHO (CHO-K1) cells and the GAG-deficient CHO cells (pgsA-745) were cultured in nutrient F-12 Ham (Sigma, St. Louis, MO) supplemented with 10% heat-inactivated fetal bovine serum (FBS; Lonza Group, Basel, Switzerland), which is referred to as "culture medium" hereafter, at 37 °C in an atmosphere containing 5% CO_2.

2.8. Confocal laser scanning microscopy (CLSM) observation

CLSM observation by z-stack imaging mode was performed using an LSM 800 (Carl Zeiss, Oberkochen, Germany) with a C-Apochromat 40 ×/1.20 W Korr objective at an excitation wavelength of 488 nm (Ar laser) for the visualization of FAM-labeled peptide. The nuclei of cells counterstained with Hoechst were excited at an excitation wavelength of 405 nm. In the CLSM experiment, the detection pinhole diameter was set to be 1.0 times of the diameter of the Airy Disk, resulting in a thickness of the optical sections of < 1.0 μm. This optical thickness was sufficiently small relative to the thickness of the cells used in this study. In addition, the z-stack imaging acquires a number of optical slice images from the periphery of the cells attached onto glass bottom dish toward the opposite periphery by scanning every 0.38 μm. These conditions ensured that the detected fluorescence of FAM-labeled peptides is at the same plane of focus as the nuclear stain, validating that the peptides remain within the cell (Fig. S1). Cells (2.0×10^5 cells) were plated in 35 mm glass-bottom dishes coated with poly(L-lysine) (Matsunami Glass, Osaka, Japan) and were incubated in culture medium. After incubation for 24 h (37 °C, 5% CO_2), the cells were incubated with FAM-labeled peptides for 30 min at 4 °C or for 10 min at 37 °C in FBS-free F12-Ham medium. Regarding the cells incubated with FAM-Rev at 37 °C, the incubation time was extended to 30 min. After the incubation, the cells were washed 3 times with phosphate-buffered saline (PBS) on ice, and kept in PBS, followed by confocal microscopic imaging. The nuclei were labeled with Hoechst 33342 (Life Technologies, Waltham, MA) by following the manufacturer's instructions. For the GUV observations, GUV suspension was incubated with 0.1 μM of FAM-labeled peptides in 10 mM Tris buffer (pH 7.4) containing 10 mM glucose at room temperature for 10 min on a bovine serum albumin-coated glass bottom dish (Matsunami Glass).

2.9. Quantification of cell membrane penetration of peptides by flow cytometric analysis

The amount of membrane penetration of peptide was quantified by a modified version of the flow cytometric method established in previous studies [28,29]. Cells were seeded into 24-well plates at a density of 1.0×10^5 cells/well and incubated in culture medium. After incubation for 24 h (37 °C, 5% CO_2), the cells were washed with PBS and incubated with 0.5–2.0 μM FAM-labeled peptides for 30 min at 4 °C in 250 μL/well FBS-free F12-Ham medium. The cells were then washed with PBS and incubated for 5 min at 37 °C with 0.25% trypsin-EDTA (250 μL/well) purchased from Life Technologies. Subsequently, 250 μL of PBS containing FBS was added and the cells were gently suspended and the supernatant after centrifugation at 2500 rpm for 2 min was carefully removed. By the centrifugation, the supernatant was removed 2 times. The resultant cell pellet was then further washed 3 times with 500 μL of PBS containing 2% FBS, and was resuspended in 500 μL of PBS containing 2% FBS, followed by a 25 μm-meshed filter (BD Falcon). As a control, cells that were not incubated with FAM-labeled peptides were also analyzed. FAM fluorescence was detected at an excitation wavelength of 488 nm and monitored with 530/30 bandpass filter on a FACS-Calibur flow cytometer (BD Biosciences). Each sample was run in triplicate (3 × 10,000 events). Events corresponding to cellular debris were removed by gating on forward and side scatter. Mean fluorescence values were determined from the histograms using Cell Quest Pro software.

2.10. Statistical analysis

The statistical differences in the collected data were evaluated using one-way analysis of variance followed by Dunnett's test (Fig. 4B, Fig. S9) or Bonferroni's test (Fig. 6B), by means of Prism software (GraphPad Software, La Jolla, CA). We set the level of significance at $P < 0.05$.

3. Results

3.1. Design of amphipathic arginine-rich peptides

A newly designed amphipathic arginine-rich peptide, A2-17, is shown in Fig. 1. To investigate the effect of arginine residues on the cell membrane penetration ability of A2-17, we also designed an A2-17 derivative, A2-17KR, by substituting all lysine residues in A2-17 with arginine residues (Fig. 1). The value for the hydrophobic moment in each peptide with α-helical structure, ⟨μH⟩, as a measure of the amphipathicity, was calculated by the Eisenberg scale [30,31], showing that the amphipathicity of A2-17 and A2-17KR is much larger than that of Rev.

3.2. GAG interaction

First we examined the secondary structure of A2-17 variants bound to heparin by Far-UV CD measurements because of the possibility that the α-helix formation of arginine-rich peptide influences its cell membrane penetration efficiency [15,32]. Far-UV CD spectra of A2-17 and A2-17KR as well as Rev in the presence of heparin are shown in Fig. 2A. In contrast to the CD spectra corresponding to a predominant random coil structure in the absence of heparin (Fig. S2A), typical CD spectra of α-helical structure with double minima near 208 and 222 nm were observed for all peptides bound to heparin. The calculated α-helix contents for Rev, A2-17, and A2-17KR bound to heparin were 40%, 54%, and 78%, respectively, indicating that A2-17 variants, especially A2-17KR have greater tendency to form α-helical structure than Rev upon binding to GAGs.

We previously showed that the favorable enthalpy gain of arginine-rich peptides upon binding to GAGs provides energetic source to

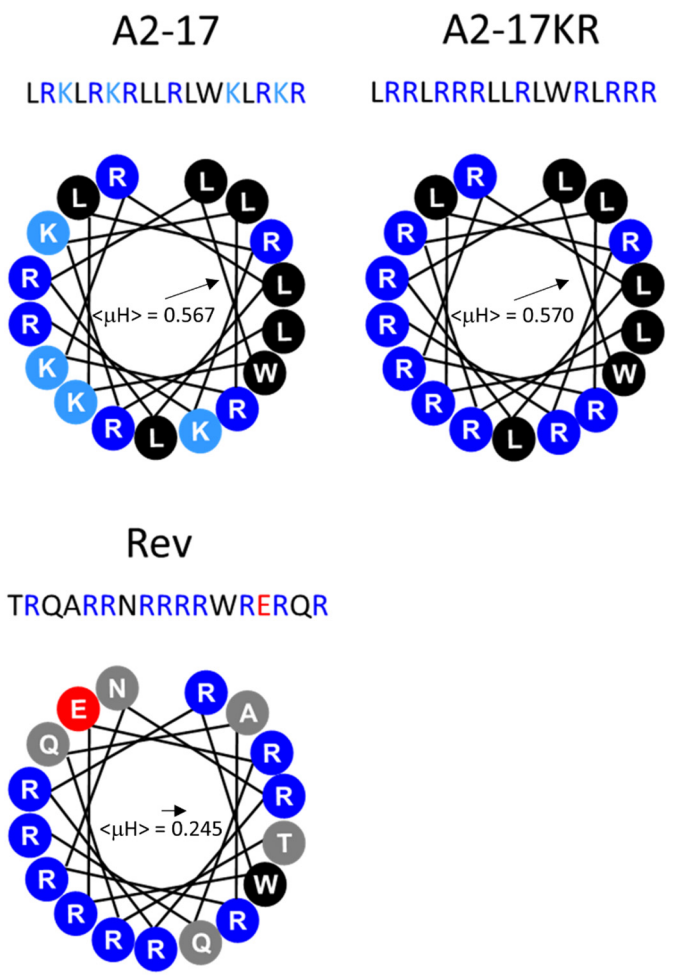

Fig. 1. Helical wheel diagrams for amino acid sequences of A2-17, A2-17KR, and Rev arranged as an ideal α-helix (100° rotation per residue) seen down the long axis from the amino terminal end. The hydrophobic moment ⟨μH⟩, as a measure of amphipathicity of α-helix, for A2-17, A2-17KR, and Rev is calculated to be 0.567, 0.570, and 0.245, respectively, on the Eisenberg scale. The arrows indicate direction of polarization of residues in the hydrophobic moment.

promote their cell penetration [15]. Thus, the interaction of A2-17 variants with heparin was next investigated by ITC measurements. Similarly to the case of Rev binding to heparin [15], large exothermic heats upon binding of A2-17 to heparin were observed (Fig. 2B), and the heats of reaction were analyzed according to the one-site binding model (Fig. 2C). The resultant thermodynamic parameters were summarized in Table 1. The binding enthalpy ($\Delta H^{\circ} = -6.3$ kcal/mol) and the binding constant ($K = 3.3 \times 10^{7}\ M^{-1}$) of A2-17 were found to be about half of the corresponding values for Rev (Table 1). Given the numbers of arginine residues in A2-17 and Rev peptides are 6 and 10, respectively, this result is consistent with the previous finding that the enthalpic contribution to the strong affinity of arginine-rich peptides for heparin is largely derived from the favorable electrostatic interaction between arginine residues of peptide and anionic sulfate/carboxyl groups of heparin [15]. Indeed, the binding enthalpy and binding constant of A2-17KR (the number of arginine residues is 10) in which all lysine residues in A2-17 are substituted with arginine residues to heparin were much larger than those of A2-17 (Fig. 2C and Table 1). It should be noted that the heparin-binding nature of cationic peptides would be largely derived from the electrostatic interaction between arginine/lysine residues of peptide and anionic sulfate/carboxyl groups of heparin [10,15,24,33,34]. Consistently, the binding stoichiometry in charge neutralization for all peptides is around 8–11 peptides per

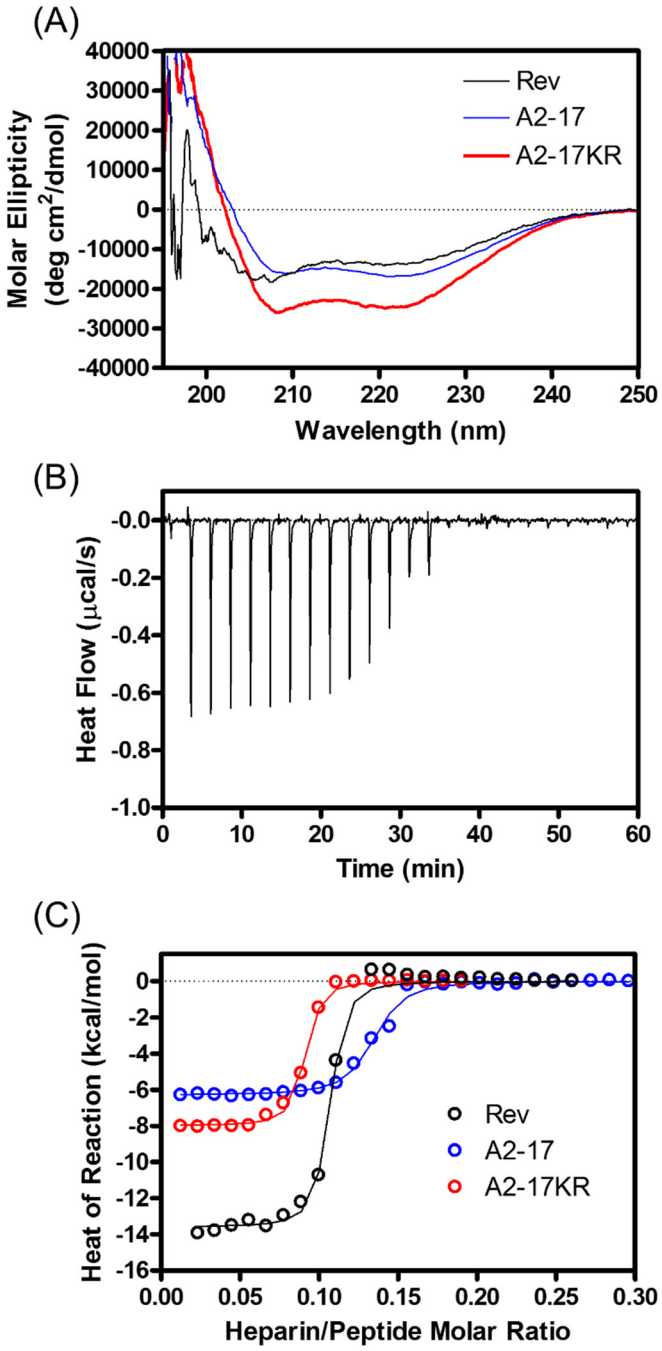

Fig. 2. (A) Far-UV CD spectra of Rev (black line), A2-17 (blue line), and A2-17KR (red line) in the presence of heparin. Peptide and heparin concentrations were 0.1 and 0.16 mg/ml, respectively. (B) ITC thermogram for heparin (100 μM) injection into A2-17 (45 μM) in 10 mM Tris buffer containing 150 mM NaCl. Each peak in heat flow chart corresponds to the injection of 1.0 μL aliquots of heparin. (C) The heats of reaction for the binding were plotted as a function of the heparin/peptide molar ratio. The lines are the best fit curves to the experimental data using one-site binding model. The result of Rev is from our previous study [15]. (For interpretation of the references to color in this figure legend, the reader is referred to the web version of this article.)

heparin (mol/mol) (Table 1), indicating that negative charges in the heparin molecule used was neutralized by binding of 8–11 peptides that have 10 arginine/lysine positive charges in the peptide molecule. We note that such charge neutralization would induce the formation of large peptide–heparin complexes/aggregates, as actually seen in the light scattering measurements (Fig. S3, inset).

Table 1
Thermodynamic parameters for binding of peptides to heparin at 25 °C.

	Binding stoichiometry (peptide/heparin, mol/mol)	K (M^{-1})	$\Delta G°$[a] (kcal/mol)	$\Delta H°$ (kcal/mol)	$T\Delta S°$[b] (kcal/mol)
Rev[c]	9.8 ± 0.5	$(7.0 \pm 3.0) \times 10^7$	−10.6 ± 0.25	−13.9 ± 0.76	−3.3 ± 0.94
A2-17	7.7 ± 0.25	$(3.3 \pm 0.64) \times 10^7$	−10.2 ± 0.11	−6.3 ± 0.20	3.9 ± 0.11
A2-17KR	11.4 ± 0.25	$(7.3 \pm 1.6) \times 10^7$	−10.7 ± 0.13	−8.1 ± 0.50	2.6 ± 0.13

[a] Gibbs free energy of binding was calculated according to $\Delta G° = -RT \ln K$.
[b] The entropy of binding was calculated from $\Delta G° = \Delta H° - T\Delta S°$.
[c] Data are from our previous study [15].

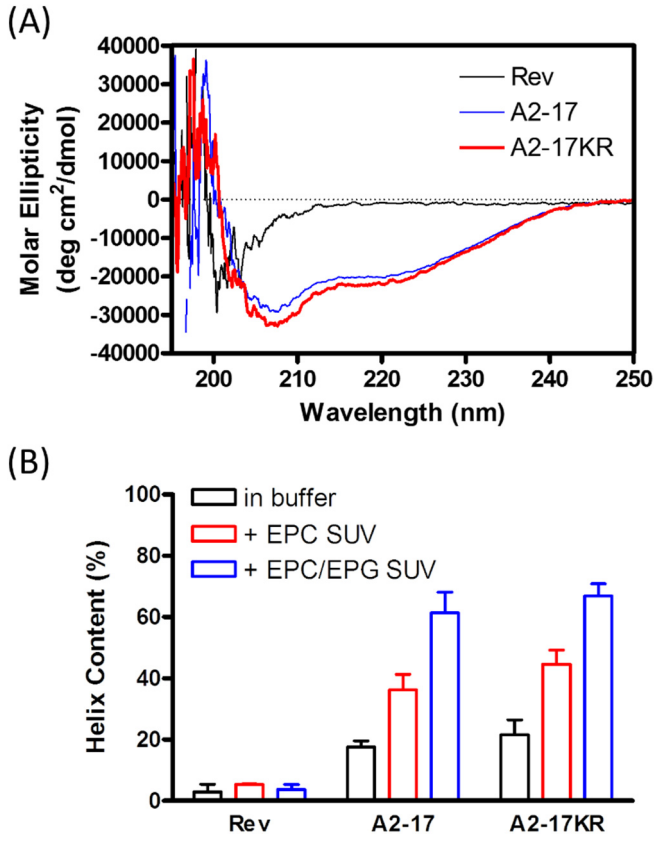

Fig. 3. (A) Far-UV CD spectra of Rev (black line), A2-17 (blue line), and A2-17KR (red line) in the presence of EPC/EPG (4/1) SUVs. Peptide and phospholipid concentrations were 0.05 and 1.0 mg/ml, respectively. (B) The α-helix content of peptide in the absence (black column) and the presence of EPC SUVs (red column) or EPC/EPG SUVs (blue column). (For interpretation of the references to color in this figure legend, the reader is referred to the web version of this article.)

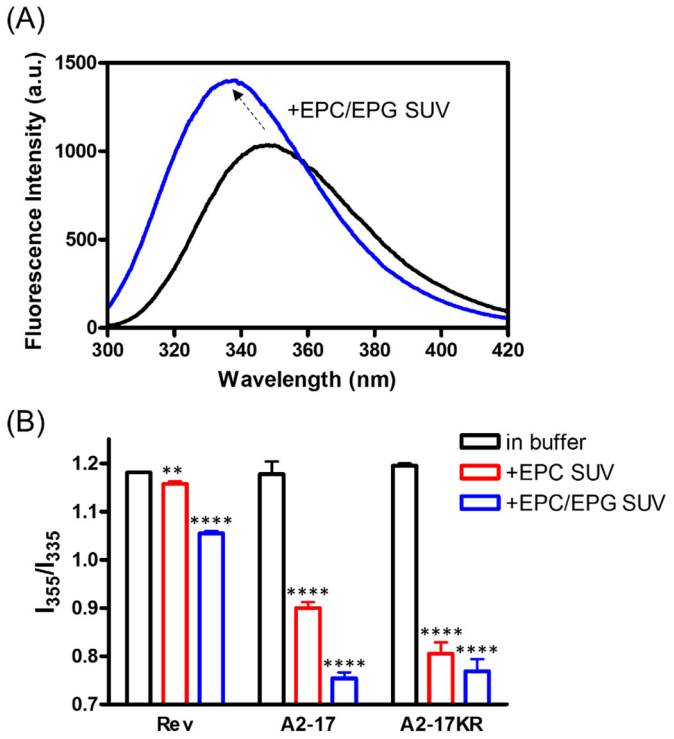

Fig. 4. (A) Trp fluorescence spectra for A2-17 in buffer (black line) and in the presence of EPC/EPG (4/1) SUVs (blue line). Peptide and phospholipid concentrations were 0.05 and 1.0 mg/ml, respectively. (B) Comparison of fluorescence intensity ratios at 355/335 nm for peptides in the absence (black column) and the presence of EPC SUVs (red column) or EPC/EPG SUVs (blue column). **, $P < 0.01$ versus "in buffer"; ****, $P < 0.0001$ versus "in buffer" by Dunnett's test. (For interpretation of the references to color in this figure legend, the reader is referred to the web version of this article.)

3.3. Lipid membrane interaction

To investigate the ability of A2-17 variants to form α-helical structure upon binding to lipid membranes, we further performed CD measurements of peptides in the presence of anionic EPC/EPG (4/1) SUVs. As shown in Fig. 3A, both A2-17 and A2-17KR exhibited typical CD spectra for α-helical structure upon binding to EPC/EPG SUVs, whereas Rev exhibited a random coil structure. Similar but less pronounced effects of lipid binding on the CD spectra of peptides were seen in the binding to neutral EPC SUVs (Fig. S2B). Fig. 3B summarizes the α-helix contents of peptides upon binding to SUVs. A2-17 and A2-17KR have a great ability to form α-helical structure upon binding not only to EPC/EPG SUVs but also to neutral EPC SUVs. In contrast, Rev exhibited no such α-helix formation in the presence of any SUVs, indicating that Rev does not form α-helical structure upon binding to lipid membranes [15,35]. Thus, these results imply that A2-17 and A2-17KR have the strong affinity for lipid membranes.

Next, we examined the change in Trp fluorescence spectra of arginine-rich peptides upon binding to SUVs since all peptides have one Trp residue at position 12 (Fig. 1). A significant blue shift of wavelength of maximum fluorescence together with an increase in fluorescence intensity of Trp fluorescence spectra was observed for A2-17 in the presence of EPC/EPG SUVs (Fig. 4A), indicating the transfer of Trp residue in peptide from aqueous phase to a more hydrophobic environment in lipid membranes. As shown in Fig. 4B, both A2-17 and A2-17KR exhibited marked decreases in I_{355}/I_{335} upon binding to EPC/EPG SUVs, and even to neutral EPC SUVs, in contrast to the case of Rev. These results clearly indicate that A2-17 and A2-17KR have the greater ability than Rev to bind to the membrane surface with inserting into the hydrophobic interiors of lipid membranes. In agreement with this, FAM-labeled A2-17 and A2-17KR exhibited strong fluorescence signals in the membrane regions of EPC/EPG GUVs compared to FAM-labeled Rev in the CLSM observations (Fig. S4).

We further analyzed the membrane binding nature of A2-17 and A2-

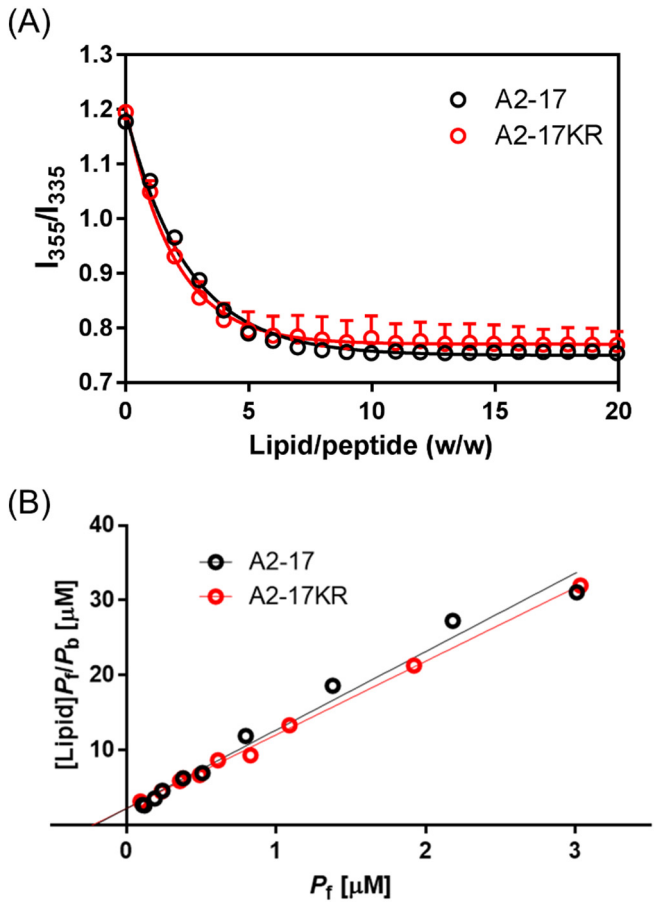

Fig. 5. (A) Changes in fluorescence intensity ratio at 355/335 nm of Trp residue in A2-17 (black circle) and A2-17KR (red circle) as a function of weight ratio of total lipids of EPC/EPG (4/1) SUVs to peptide. (B) Hanes-Woolf plot analysis for the binding data of A2-17 (black circle) and A2-17KR (red circle). The solid lines represent the linear regression. (For interpretation of the references to color in this figure legend, the reader is referred to the web version of this article.)

Table 2
Thermodynamic parameters for binding of peptides to EPC/EPG (4/1) and EPC lipid membranes at 25 °C.

Lipid membrane	Peptide	Binding stoichiometry (peptide/lipid, mol/mol)	K (M^{-1})	$\Delta G°$[a] (kcal/mol)
EPC/EPG	Rev[b]	0.013 ± 0.0010	(1.2 ± 0.40) × 10^4	−5.0 ± 0.20
	A2-17	0.088 ± 0.013	(5.2 ± 1.86) × 10^6	−9.1 ± 0.21
	A2-17KR	0.10 ± 0.013	(4.2 ± 1.41) × 10^6	−9.0 ± 0.21
EPC	A2-17	0.064 ± 0.016	(0.91 ± 0.35) × 10^6	−8.1 ± 0.22
	A2-17KR	0.064 ± 0.017	(1.5 ± 0.27) × 10^6	−8.4 ± 0.10

[a] Gibbs free energy of binding was calculated according to $\Delta G° = -RT \ln K$.
[b] Data are from our previous study [15].

17KR from the change in I_{355}/I_{335} of Trp fluorescence according to the one-site binding model (Fig. 5; see also Materials and Methods). This approach is useful to obtain binding parameters when ITC analysis is difficult to be conducted due to the complicated behavior of heat reaction caused by the interaction of amphipathic peptides with lipid membranes such as vesicle aggregation. By using the titration data of A2-17 variants with EPC/EPG SUVs (Fig. 5A), the binding constant, K and the maximal binding capacity, B_{max} values were obtained from the linear regression (Fig. 5B). As summarized in Table 2, A2-17 and A2-17KR exhibited similar binding constant of ~5 × 10^6 M^{-1}, which are 2 orders of magnitude larger than that of Rev (1.2 × 10^4 M^{-1}) [15]. We also conducted Trp fluorescence analysis for binding of A2-17 to heparin (Fig. S3 and Table S1), confirming that Trp fluorescence measurements give the comparable binding parameters to those obtained by ITC measurements (Table 1).

It should be noted that if the binding of peptides to the lipid membrane surface is only driven by the electrostatic interaction between the positively charged residues of peptide and the negatively charged PG molecules in the membrane surface, the value of binding stoichiometry is expected to be 0.01, which corresponds to the equivalent ratio of the positively charged residues of peptide (10 of arginine and lysine residues) to the negatively charged PG molecules in the outer leaflet of EPC/EPG (4/1) SUVs (10 mol% of total lipids). Indeed, the binding stoichiometry for Rev is almost the same to the expected value of 0.01 (Table 2), indicating that the binding of Rev to the membrane surface is mainly driven by electrostatic interaction. In contrast, the binding stoichiometry values for A2-17 and A2-17KR (molar ratio of peptide/lipid ~0.1) are much greater than that for Rev (Table 2). This indicates that the stronger binding of A2-17 and A2-17KR than Rev to the lipid membranes is derived not only from electrostatic interaction but also from van der Waals and hydrophobic interactions between amphipathic α-helix of peptides and hydrophobic interior of lipid membranes. To support this idea, A2-17 and A2-17KR exhibited notable binding to neutral EPC SUVs (Figs. 4B and S5), and the resulting binding parameters indicated that A2-17 and A2-17KR have comparable binding constants and stoichiometries to EPC SUVs compared to those to EPC/EPG (4/1) SUVs (Table 2).

3.4. Cell membrane penetration

Cell membrane penetration of peptides was examined in CHO-K1 cells at 4 °C, at which cellular uptake by endocytosis is inhibited [36]. CLSM images clearly demonstrated that at a low concentration (2 μM) of added peptides, A2-17 and A2-17KR efficiently penetrated cell membranes, whereas Rev exhibited little cell membrane penetration (Fig. 6A). Consistently, flow cytometric analysis quantified approximately 10 times larger amount of cell-associated and internalized peptides for A2-17 and A2-17KR compared to that of Rev (Fig. 6B). It should be noted that high peptide concentrations (typically > 10 μM) are usually prerequisite for efficient cell membrane penetration of arginine-rich cell-penetrating peptides [37]. Indeed, a significant cell membrane penetration of Rev was observed at 10 μM of peptide concentration (Fig. S6). These results indicate that the increase in amphipathicity with α-helix-forming ability can enhance the cell membrane penetration even at low concentration of arginine-rich peptide. Interestingly, A2-17KR tends to exhibit lower efficiency for cell membrane penetration compared to A2-17 (Fig. 6A and B) despite of their similar amphipathicity.

4. Discussion

We have previously proposed a physicochemical process for the direct cell membrane penetration of arginine-rich peptides: the peptides bind to GAGs on the cell surface, followed by the transfer to the lipid membranes, and consequently penetrate into cells across the membranes [15,38]. To support the model, we have recently succeeded in observing the process of a fluorinated arginine-rich peptide in cells by means of real-time ^{19}F-NMR spectroscopy [39]. To achieve the effective cell membrane penetration, arginine-rich peptides bound to GAGs on the cell surface have to partition to the lipid membranes. However, since arginine-rich peptides usually have much greater binding affinity for GAGs than that for lipid membranes in a charge-density dependent manner, they are most likely to bind to GAGs on the cell surface rather than to lipid membranes [40]. In addition, the concentration gradient of peptides between the outer and inner leaflets of the membranes has to be achieved as a driving force for the membrane penetration [41].

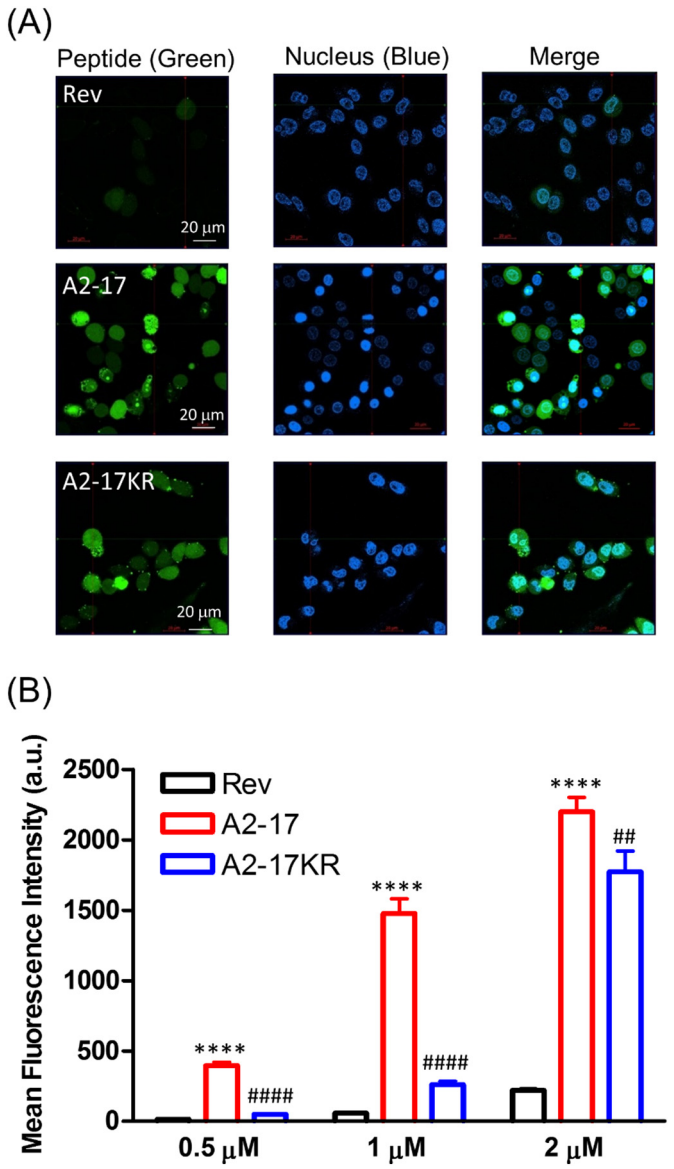

Fig. 6. (A) Confocal fluorescent images of CHO-K1 cells treated with 2 μM of FAM-labeled Rev (upper panels), A2-17 (middle panels), and A2-17KR (lower panels) at 4 °C. FAM fluorescence and Hoechst fluorescence counterstaining nuclei were shown in green and blue, respectively, together with the merged image. Scale bars represent 20 μm. (B) Flow cytometric quantification of the amount of cell-associated and internalized peptides in CHO-K1 cells at 4 °C when CHO-K1 cells were incubated with low peptide concentrations (0.5–2 μM). ****, $P < 0.0001$ versus Rev; ##, $P < 0.01$ versus A2-17; ####, $P < 0.0001$ versus A2-17 by Bonferroni's test.

These facts may explain why relatively high peptide concentrations are required for their efficient cell membrane penetration as reported in many studies [10,15,33,41–44], in which the peptide concentrations were usually over 10 μM. Indeed, Rev hardly penetrated cell membranes at 2 μM or less of peptide concentrations (Fig. 6), whereas the efficient cell membrane penetration was observed at 10 μM (Fig. S6). It should be noted that although the lipid membrane interaction is essential for the cell membrane penetration of arginine-rich peptides, their binding nature to GAGs is still critical as their initial step for the cell membrane penetration [15]. Indeed, the internalizations of A2-17 and A2-17KR into pgsA-745 cells that are CHO mutant defective in GAG biosynthesis were largely inhibited (Fig. S7), indicating the critical role of GAGs in the cell membrane penetration of the A2-17 variants [45].

A significant finding in this study is that A2-17 variants efficiently penetrate cell membranes at much lower peptide concentrations of 1–2 μM compared to Rev (Fig. 6). Despite A2-17 and Rev have the similar binding affinity for heparin, A2-17 exhibits much higher affinity and capacity for binding to lipid membranes compared to Rev, with formation of amphipathic α-helix and greater insertion into lipid membrane interiors (Tables 1 and 2, Figs. 3 and 4). Upon binding to lipid membranes, the circumferential distribution of arginine residues in Rev is likely to interfere α-helix formation because of charge repulsion (Fig. 1). In contrast, such charge repulsion from arginine residues in amphipathic A2-17 can be compensated by the free energy reduction upon lipid binding [46]. Such enhanced lipid-binding properties of A2-17 would facilitate the transfer of peptides from GAGs to lipid membranes, resulting in the efficient cell membrane penetration (Fig. 6). Alternatively, the formation of large aggregates upon binding of A2-17 to GAGs (Fig. S3) may facilitate the internalization of the peptide–GAG complexes [47].

At physiological temperature, arginine-rich peptides are thought to be uptaken into cells via endocytosis as well as the direct cell membrane penetration mechanism [8]. Indeed, we confirmed that A2-17 and A2-17KR exhibited efficient cell uptake when incubated at 37 °C (Fig. S8), indicating the ability of the A2-17 variants to penetrate cell membranes efficiently at physiological temperature. For Rev, in contrast, punctuate fluorescence pattern in the cells was observed (Fig. S8), indicating predominant endocytic uptake and remaining in endosomes, consistent with the notion that typical arginine-rich peptides are likely to be endocytosed at low peptide concentrations [37]. These results suggest that although the direct membrane penetration and endocytic uptake of arginine-rich peptides are likely to occur simultaneously at physiological temperature, the predominant mechanism is controlled depending upon the physicochemical property of the peptides [36].

It has been suggested that the secondary structure of cell-penetrating peptides on lipid membranes controls the lipid membrane interaction and insertion, thereby enhancing their cell membrane penetration [35,48]. It is known that the formation of α-helical structure decreases the polarity and the free energy cost of transfer to the hydrophobic membranes for peptide bonds in the peptide molecule [49,50]. In addition, amphipathic α-helical structure is favorable to the insertion of peptides into the lipid membrane interiors (Fig. 4), causing a membrane curvature stress with thinning and lateral compression of the membranes [51–54]. In this situation, the membrane curvature stress is likely to be eliminated by the deeper penetration of peptides into the membrane interiors with the formation of transient pores [4,55–57], resulting in the efficient membrane penetration as seen for A2-17 variants (Fig. 6). We note that although Rev and A2-17 have no cytotoxicity to CHO-K1 cells, A2-17KR exhibits cytotoxicity to some extent (Fig. S9), consistent with a recent finding that substitution of arginine residues in amphipathic peptides with lysine residues greatly reduces the cytotoxicity of peptides [58]. Although the mechanism by which arginine residue increases the cytotoxicity of amphipathic cationic peptides is unclear, strong interactions of A2-17KR with both GAGs and lipid membranes (Tables 1 and 2) might derive to disrupt cell membranes [59,60].

Interestingly, A2-17KR penetrates cell membranes less efficiently than A2-17 (Fig. 6) despite their similar binding affinity for lipid membranes (Fig. 5 and Table 2). It is possible that the membrane partitioning of A2-17KR after the GAG binding can be impeded due to the increased binding affinity for GAGs compared to A2-17 (Table 1). In addition, increased numbers of arginine residues in A2-17KR (10 arginine residues) compared to A2-17 (6 arginine residues) would enhance the enthalpic interaction of peptides with GAGs [15]. Therefore, the optimal balance between the bindings to GAGs and lipid membranes is likely to be important for the efficient cell-penetrating ability of arginine-rich peptides. It should be noted that the optimal number of arginine residues in arginine-rich peptide for the efficient cell penetration was shown to be 8–15 according to the previous studies [15,42,44,61].

In conclusion, we have developed a novel amphipathic cell-

penetrating peptide, A2-17, based on the N-terminal GAG binding region of human apolipoprotein E. Our results demonstrated that A2-17 has a strong ability to bind to GAGs as well as lipid membranes with formation of amphipathic α-helix, resulting in the efficient cell membrane penetration even at low peptide concentrations. Thus, design of amphipathic α-helical structure that increases the affinity for lipid membranes with controlling the affinity for GAGs, would be a promising strategy to enhance the cell membrane penetration of arginine-rich peptides. Although the cell internalization mechanism can be altered by the presence of cargo substances, resulting in complicated obstacles for the delivery of peptide–cargo complexes [62], we believe that the understanding of the mechanism for the cell membrane penetration of arginine-rich peptides will contribute to development of innovative strategy for delivering drug molecules [2,60,63].

Conflict of interest statements

The authors declare no conflict of interests.

Author contributions

T.O. and Y.T-H. contributed equally to this work. R.N., Karin Nishikiori, K.H., and K.A. designed and synthesized peptides. T.O. performed Trp fluorescence and CD measurements. R.N. performed ITC measurements. M.K., Y.T., and T.O. performed cell experiments. Kazuchika Nishitsuji provided statistical analyses of data. Y.T-H., Kazuchika Nishitsuji, K.U., K. S-K., and H.S. designed the study and interpreted the data, and H.S. wrote the paper. All authors reviewed the results and approved the final version of the manuscript.

Transparency document

The Transparency document associated with this article can be found, in online version.

Acknowledgements

This work was partly supported by JSPS KAKENHI Grant Numbers JP17H03979 (to H.S.) from Japan Society for the Promotion of Science and the Research on Development of New Drugs 18ak0101074h0902 from Japan Agency for Medical Research and Development, AMED.

Appendix A. Supplementary data

Thermodynamic parameters for binding of A2-17 to heparin determined by Trp fluorescence measurement (Table S1). Ortho image assembled from CLSM observation by z-stack imaging mode (Fig. S1). Far-UV CD spectra of Rev, A2-17, and A2-17KR in the absence or presence of EPC SUVs (Fig. S2). Analyses of Trp fluorescence and light scattering intensity for binding of A2-17 to heparin (Fig. S3). Confocal fluorescent images of EPC/EPG GUVs incubated with FAM-labeled Rev and A2-17 variants (Fig. S4). Trp fluorescence analysis for binding of A2-17 variants to EPC SUVs (Fig. S5). Confocal fluorescent images of CHO-K1 cells treated with 10 μM of FAM-labeled Rev (Fig. S6). Confocal fluorescent images of pgsA-745 cells treated with 2 μM of FAM-labeled A2-17 variants at 4 °C (Fig. S7). Confocal fluorescent images of CHO-K1 cells treated with 2 μM of FAM-labeled Rev and A2-17 variants at 37 °C (Fig. S8). Cytotoxicity of Rev and A2-17 variants in CHO-K1 cells (Fig. S9). Supplementary data to this article can be found online at https://doi.org/10.1016/j.bbamem.2018.12.010.

References

[1] E. Koren, V.P. Torchilin, Cell-penetrating peptides: breaking through to the other side, Trends Mol. Med. 18 (2012) 385–393.
[2] M. Rizzuti, M. Nizzardo, C. Zanetta, A. Ramirez, S. Corti, Therapeutic applications of the cell-penetrating HIV-1 Tat peptide, Drug Discov. Today 20 (2015) 76–85.
[3] Y.S. Choi, A.E. David, Cell penetrating peptides and the mechanisms for intracellular entry, Curr. Pharm. Biotechnol. 15 (2014) 192–199.
[4] H. Herce, A. Garcia, Cell penetrating peptides: how do they do it? J. Biol. Phys. 33 (2007) 345–356.
[5] H. Hirose, T. Takeuchi, H. Osakada, S. Pujals, S. Katayama, I. Nakase, S. Kobayashi, T. Haraguchi, S. Futaki, Transient focal membrane deformation induced by arginine-rich peptides leads to their direct penetration into cells, Mol. Ther. 20 (2012) 984–993.
[6] C. Palm-Apergi, A. Lorents, K. Padari, M. Pooga, M. Hällbrink, The membrane repair response masks membrane disturbances caused by cell-penetrating peptide uptake, FASEB J. 23 (2009) 214–223.
[7] B.R. Liu, Y.W. Huang, J.G. Winiarz, H.J. Chiang, H.J. Lee, Intracellular delivery of quantum dots mediated by a histidine- and arginine-rich HR9 cell-penetrating peptide through the direct membrane translocation mechanism, Biomaterials 32 (2011) 3520–3537.
[8] A. Walrant, S. Cardon, F. Burlina, S. Sagan, Membrane crossing and membranotropic activity of cell-penetrating peptides: dangerous liaisons? Acc. Chem. Res. 50 (2017) 2968–2975.
[9] S. Rehmani, J.E. Dixon, Oral delivery of anti-diabetes therapeutics using cell penetrating and transcytosing peptide strategies, Peptides 100 (2018) 24–35.
[10] H.L. Amand, H.A. Rydberg, L.H. Fornander, P. Lincoln, B. Nordén, E.K. Esbjörner, Cell surface binding and uptake of arginine- and lysine-rich penetratin peptides in absence and presence of proteoglycans, Biochim. Biophys. Acta 1818 (2012) 2669–2678.
[11] A. Ziegler, Thermodynamic studies and binding mechanisms of cell-penetrating peptides with lipids and glycosaminoglycans, Adv. Drug Deliv. Rev. 60 (2008) 580–597.
[12] R.J. Naik, A. Chatterjee, M. Ganguli, Different roles of cell surface and exogenous glycosaminoglycans in controlling gene delivery by arginine-rich peptides with varied distribution of arginines, Biochim. Biophys. Acta 1828 (2013) 1484–1493.
[13] J.E. Dixon, G. Osman, G.E. Morris, H. Markides, M. Rotherham, Z. Bayoussef, A.J. El Haj, C. Denning, K.M. Shakesheff, Highly efficient delivery of functional cargoes by the synergistic effect of GAG binding motifs and cell-penetrating peptides, Proc. Natl. Acad. Sci. U. S. A. 113 (2016) E291–E299.
[14] J.R. Fromm, R.E. Hileman, E.E.O. Caldwell, J.M. Weiler, R.J. Linhardt, Differences in the interaction of heparin with arginine and lysine and the importance of these basic amino acids in the binding of heparin to acidic fibroblast growth factor, Arch. Biochem. Biophys. 323 (1995) 279–287.
[15] Y. Takechi-Haraya, R. Nadai, H. Kimura, K. Nishitsuji, K. Uchimura, K. Sakai-Kato, K. Kawakami, A. Shigenaga, T. Kawakami, A. Otaka, H. Hojo, N. Sakashita, H. Saito, Enthalpy-driven interactions with sulfated glycosaminoglycans promote cell membrane penetration of arginine peptides, Biochim. Biophys. Acta 1858 (2016) 1339–1349.
[16] J. Chen, Q. Li, J. Wang, Topology of human apolipoprotein E3 uniquely regulates its diverse biological functions, Proc. Natl. Acad. Sci. U. S. A. 108 (2011) 14813–14818.
[17] M.C. Phillips, Apolipoprotein E isoforms and lipoprotein metabolism, IUBMB Life 66 (2014) 616–623.
[18] M. Zaiou, K.S. Arnold, Y.M. Newhouse, T.L. Innerarity, K.H. Weisgraber, M.L. Segall, M.C. Phillips, S. Lund-Katz, Apolipoprotein E—low density lipoprotein receptor interaction influences of basic residue and amphipathic alpha-helix organization in the ligand, J. Lipid Res. 41 (2000) 1087–1095.
[19] H. Saito, P. Dhanasekaran, D. Nguyen, F. Baldwin, K.H. Weisgraber, S. Wehrli, M.C. Phillips, S. Lund-Katz, Characterization of the heparin binding sites in human apolipoprotein E, J. Biol. Chem. 278 (2003) 14782–14787.
[20] A. Sivashanmugan, J. Wang, A unified scheme for initiation and conformational adaptation of human apolipoprotein E N-terminal domain upon lipoprotein binding and for receptor binding activity, J. Biol. Chem. 284 (2009) 14657–14666.
[21] E. Leupold, H. Nikolenko, M. Beyermann, M. Dathe, Insight into the role of HSPG in the cellular uptake of apolipoprotein E-derived peptide micelles and liposomes, Biochim. Biophys. Acta 1778 (2008) 2781–2789.
[22] H. Saito, P. Dhanasekaran, D. Nguyen, E. Deridder, P. Holvoet, S. Lund-Katz, M.C. Phillips, Alpha-helix formation is required for high affinity binding of human apolipoprotein A-I to lipids, J. Biol. Chem. 279 (2004) 20974–20981.
[23] A. Ziegler, X.L. Blatter, A. Seelig, J. Seelig, Protein transduction domains of HIV-1 and SIV TAT interact with charged lipid vesicles. Binding mechanism and thermodynamic analysis, Biochemistry 42 (2003) 9185–9194.
[24] G. Klocek, J. Seelig, Melittin interaction with sulfated cell surface sugars, Biochemistry 47 (2008) 2841–2849.
[25] J.M. Scholtz, H. Qian, E.J. York, J.M. Stewart, R.L. Baldwin, Parameters of helix-coil transition theory for alanine-based peptides of varying chain lengths in water, Biopolymers 31 (1991) 1463–1470.
[26] Ø. Strømland, Ø.S. Handegård, M.L. Govasli, H. Wen, Ø. Halskau, Peptides derived from α-lactalbumin membrane binding helices oligomerize in presence of lipids and disrupt bilayers, Biochim. Biophys. Acta 1859 (2017) 1029–1039.
[27] M. Kono, Y. Okumura, M. Tanaka, D. Nguyen, P. Dhanasekaran, S. Lund-Katz, M.C. Phillips, H. Saito, Conformational flexibility of the N-terminal domain of apolipoprotein A-I bound to spherical lipid particles, Biochemistry 47 (2008) 11340–11347.
[28] A. Manceur, A. Wu, J. Audet, Flow cytometric screening of cell-penetrating peptides for their uptake into embryonic and adult stem cells, Anal. Biochem. 364 (2007) 51–59.
[29] Y.A. Nagel, P.S. Raschle, H. Wennemers, Effect of preorganized charge-display on the cell-penetrating properties of cationic peptides, Angew. Chem. Int. Ed. 56 (2017) 122–126.

[30] D. Eisenberg, E. Schwarz, M. Komaromy, R. Wall, Analysis of membrane and surface protein sequences with the hydrophobic moment plot, J. Mol. Biol. 179 (1984) 125–142.
[31] D. Eisenberg, R.M. Weiss, T.C. Terwilliger, The hydrophobic moment detects periodicity in protein hydrophobicity, Proc. Natl. Acad. Sci. U. S. A. 81 (1984) 140–144.
[32] A. Tchoumi Neree, P.T. Nguyen, D. Chatenet, A. Fournier, S. Bourgault, Secondary conformational conversion is involved in glycosaminoglycans-mediated cellular uptake of the cationic cell-penetrating peptide PACAP, FEBS Lett. 588 (2014) 4590–4596.
[33] C. Bechara, M. Pallerla, Y. Zaltsman, F. Burlina, I.D. Alves, O. Lequin, S. Sagan, Tryptophan within basic peptide sequences triggers glycosaminoglycan- dependent endocytosis, FASEB J. 27 (2013) 738–749.
[34] E. Gonçalves, E. Kitas, J. Seelig, Binding of oligoarginine to membrane lipids and heparan sulfate: structural and thermodynamic characterization of a cell-penetrating peptide, Biochemistry 44 (2005) 2692–2702.
[35] E. Eiríksdóttir, K. Konate, U. Langel, G. Divita, S. Deshayes, Secondary structure of cell-penetrating peptides controls membrane interaction and insertion, Biochim. Biophys. Acta 1798 (2010) 1119–1128.
[36] C.Y. Jiao, D. Delaroche, F. Burlina, I.D. Alves, G. Chassaing, S. Sagan, Translocation and endocytosis for cell-penetrating peptide internalization, J. Biol. Chem. 284 (2009) 33957–33965.
[37] R. Brock, The uptake of arginine-rich cell-penetrating peptides: putting the puzzle together, Bioconjug. Chem. 25 (2014) 863–868.
[38] Y. Takechi-Haraya, H. Saito, Current understanding of physicochemical mechanisms for cell membrane penetration of arginine-rich cell penetrating peptides: role of glycosaminoglycan interactions, Curr. Protein Pept. Sci. 19 (2018) 623–630.
[39] Y. Takechi-Haraya, K. Aki, Y. Tohyama, Y. Harano, T. Kawakami, H. Saito, E. Okamura, Glycosaminoglycan binding and non-endocytic membrane translocation of cell-permeable octaarginine monitored by real-time in-cell NMR spectroscopy, Pharmaceuticals 10 (2017) 42.
[40] L.E. Prevette, N.C. Benish, A.R. Schoenecker, K.J. Braden, Cell-penetrating compounds preferentially bind glycosaminoglycans over plasma membrane lipids in a charge density- and stereochemistry-dependent manner, Biophys. Chem. 207 (2015) 40–50.
[41] R. Wallbrecher, T. Ackels, R.A. Olea, M.J. Klein, L. Caillon, J. Schiller, P.H. Bovée-Geurts, T.H. van Kuppevelt, A.S. Ulrich, M. Spehr, M.J.W. Adjobo-Hermans, R. Brock, Membrane permeation of arginine-rich cell-penetrating peptides independent of transmembrane potential as a function of lipid composition and membrane fluidity, J. Control. Release 256 (2017) 68–78.
[42] S. Futaki, T. Suzuki, W. Ohashi, T. Yagami, S. Tanaka, K. Ueda, Y. Sugiura, Arginine-rich peptides. An abundant source of membrane-permeable peptides having potential as carriers for intracellular protein delivery, J. Biol. Chem. 276 (2001) 5836–5840.
[43] J.M. Gump, R.K. June, S.F. Dowdy, Revised role of glycosaminoglycans in TAT protein transduction domain-mediated cellular transduction, J. Biol. Chem. 285 (2010) 1500–1507.
[44] D.J. Mitchell, D.T. Kim, L. Steinman, C.G. Fathman, J.B. Rothbard, Polyarginine enters cells more effciently than other polycationic homopolymers, J. Pept. Res. 56 (2000) 318–325.
[45] J. Pae, L. Liivamägi, D. Lubenets, P. Arukuusk, Ü. Langel, M. Pooga, Glycosaminoglycans are required for translocation of amphipathic cell-penetrating peptides across membranes, Biochim. Biophys. Acta 1858 (2016) 1860–1867.
[46] A.S. Ladokhin, S.H. White, Folding of amphipathic α-helices on membranes: energetics of helix formation by melittin, J. Mol. Biol. 285 (1999) 1363–1369.
[47] M. Belting, Heparan sulfate proteoglycan as a plasma membrane carrier, Trends Biochem. Sci. 28 (2003) 145–151.
[48] Y. Takechi, H. Yoshii, M. Tanaka, T. Kawakami, S. Aimoto, H. Saito, Physicochemical mechanism for the enhanced ability of lipid membrane penetration of polyarginine, Langmuir 27 (2011) 7099–7107.
[49] S.H. White, W.C. Wimley, Membrane protein folding and stability: physical principles, Annu. Rev. Biophys. Biomol. Struct. 28 (1999) 319–365.
[50] P.F. Almeida, A.S. Ladokhin, S.H. White, Hydrogen-bond energetics drive helix formation in membrane interfaces, Biochim. Biophys. Acta 1818 (2012) 178–182.
[51] X. Chen, F. Sa'adedin, B. Deme, P. Rao, J. Bradshaw, Insertion of TAT peptide and perturbation of negatively charged model phospholipid bilayer revealed by neutron diffraction, Biochim. Biophys. Acta 1828 (2013) 1982–1988.
[52] J.E. Shaw, R.F. Epand, J.C.Y. Hsu, G.C.H. Mo, R.M. Epand, C.M. Yip, Cationic peptide-induced remodelling of model membranes: direct visualization by in situ atomic force microscopy, J. Struct. Biol. 162 (2008) 121–138.
[53] M. Di Pisa, G. Chassaing, J.M. Swiecicki, Translocation mechanism(s) of cell-penetrating peptides: biophysical studies using artificial membrane bilayers, Biochemistry 54 (2015) 194–207.
[54] G. Drin, B. Antonny, Amphipathic helices and membrane curvature, FEBS Lett. 584 (2010) 1840–1847.
[55] H.D. Herce, A.E. Garcia, Molecular dynamics simulations suggest a mechanism for translocation of the HIV-1 TAT peptide across lipid membranes, Proc. Natl. Acad. Sci. U. S. A. 104 (2007) 20805–20810.
[56] H.D. Herce, A.E. Garcia, J. Litt, R.S. Kane, P. Martin, N. Enrique, A. Rebolledo, V. Milesi, Arginine-rich peptides destabilize the plasma membrane, consistent with a pore formation translocation mechanism of cell-penetrating peptides, Biophys. J. 97 (2009) 1917–1925.
[57] H.D. Herce, A.E. Garcia, M.C. Cardoso, Fundamental molecular mechanism for the cellular uptake of guanidinium-rich molecules, J. Am. Chem. Soc. 136 (2014) 17459–17467.
[58] X. Meng, T. Li, Y. Zhao, C. Wu, CXC-mediated cellular uptake of miniproteins: forsaking “arginine magic”, ACS Chem. Biol. 13 (2018) 3078–3086.
[59] Y. Shai, Mechanism of the binding, insertion and destabilization of phospholipid bilayer membranes by alpha-helical antimicrobial and cell non-selective membrane-lytic peptides, Biochim. Biophys. Acta 1462 (1999) 55–70.
[60] W.B. Kauffman, T. Fuselier, J. He, W.C. Wimley, Mechanism matters: a taxonomy of cell penetrating peptides, Trends Biochem. Sci. 40 (2015) 749–764.
[61] P.A. Wender, D.J. Mitchell, K. Pattabiraman, E.T. Pelkey, L. Steinman, J.B. Rothbard, The design, synthesis, and evaluation of molecules that enable or enhance cellular uptake: peptoid molecular transporters, Proc. Natl. Acad. Sci. U. S. A. 97 (2000) 13003–13008.
[62] M. Zorko, Ü. Langel, Cell-penetrating peptides: mechanism and kinetics of cargo delivery, Adv. Drug Deliv. Rev. 57 (2005) 529–545.
[63] D.M. Copolovici, K. Langel, E. Eriste, Ü. Langel, Cell-penetrating peptides: design, synthesis, and applications, ACS Nano 8 (2014) 1972–1994.